

Electronic Supporting Information

Electrical modulation of photonic crystal band-edge laser with graphene monolayer

Hanbit Kim,^{a,b} Myungjae Lee,^{a,b} Hyunhak Jeong,^a Min-Soo Hwang,^c Ha-Reem Kim,^c

*Seondo Park,^a Yun Daniel Park,^{a,d} Takhee Lee,^{a,d} Hong-Gyu Park,^{c,e} and Heonsu Jeon^{*a,b,d}*

^a Department of Physics and Astronomy, Seoul National University, Seoul 08826, Republic of Korea

^b Inter-University Semiconductor Research Center, Seoul National University, Seoul 08826, Republic of Korea

^c Department of Physics, Korea University, Seoul 02841, Republic of Korea

^d Institute of Applied Physics, Seoul National University, Seoul 08826, Republic of Korea

^e KU-KIST Graduate School of Converging Science and Technology, Korea University, Seoul 02841, Republic of Korea

*To whom correspondence should be addressed. E-mail: hsjeon@snu.ac.kr

Device fabrication

Device fabrication began with the deposition of a 50-nm-thick Si_3N_4 hardmask layer on a semiconductor epistructure, composed of a 230-nm-thick InGaAsP multi-quantum well layer and a 1000-nm-thick InP sacrificial layer, using plasma-enhanced chemical vapor deposition (PE-CVD) method. An array of honeycomb-lattice PhC patterns were generated by electron-beam lithography. The distance between the two nearest air-holes was 450 nm while the air-hole radius was $0.32a$. The size of each PhC pattern was $\sim 18 \times 18 \mu\text{m}^2$. The PhC patterns were transferred down to the Si_3N_4 and MQW layers sequentially by reactive-ion etch (RIE) using the gas mixtures of O_2/CF_4 and CH_4/H_2 , respectively. Then, wet-etching was performed at 4°C using hydrochloric acid aqueous solution (3:1) to selectively remove the InP sacrificial layer, which resulted in a completed PBE laser sample in a free-standing membrane form. Next, a 60-nm-thick SiO_2 spacer layer was deposited on the sample by PE-CVD.

A monolayer graphene sheet, which was grown on a Cu foil by thermal chemical vapor deposition (T-CVD) method, was procured commercially from Graphene Square. After a PMMA layer was spin-coated directly on the graphene sheet as a temporary handling layer, we removed the Cu foil in a FeCl_3 solution to obtain in a free-standing PMMA/graphene film floating on water. The PMMA/graphene film was then transferred onto the PBE laser sample. The PMMA layer was removed with acetone, and dried by the critical point drying (CPD) method to prevent the suspended portions of the graphene sheet on the PhC membrane from being damaged by surface tension during the drying process. The Ti/Au (15/200 nm) gate electrodes were deposited on both the graphene surface of the sample and also on the glass substrate by electron-gun evaporator. Then, the PBE laser sample was bonded on the glass substrate using epoxy, and the graphene sheet on the sample and one of the electrodes on the glass substrate were electrically connected to each other using carbon paste. Finally, an ion-gel film for electrolyte gating was transferred and bonded on the fabricated device.

Ion-gel preparation

The ion-gel film was synthesized following the literature.¹ Briefly, an ion-gel solution was prepared first by dissolving poly (vinylidene fluoride-co-hexafluoropropylene), P(VDF-HFP), as the polymer, and 1-ethyl-3-methylimidazolium bis(trifluoromethylsulfonyl)amide, [EMI][TFSA], as the ion liquid, in acetone in a weight ratio of 1:4:7. In the P(VDF-HFP) polymer, the PHFP block is selectively dissolved in the ion liquid whereas the PVDF block is not, making the ion-gel solution gelled. After the ion-gel solution was spin-coated on a substrate to form an ion-gel film, it was cured in a vacuum oven at 80°C for 24 hours to remove the residual solvent. The completed ion-gel film was cut into an appropriate size using a razor blade, which was then transferred onto the fabricated device using a tweezer.

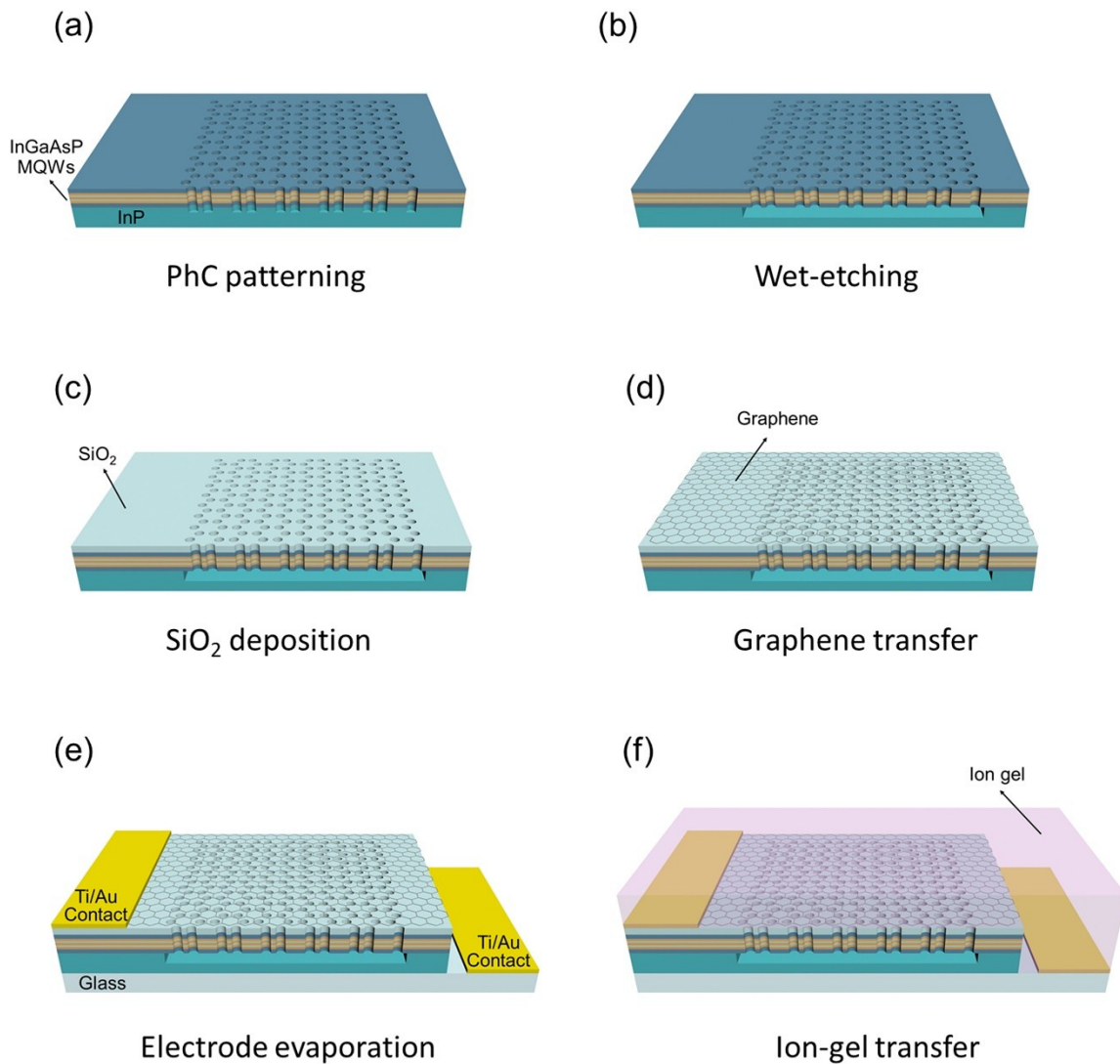


Figure S1. Fabrication steps for the PhC band-edge laser device. (a) Patterning and etching of PhC patterns on the InGaAsP MQW slab by e-beam lithography and RIE. (b) Selective wet-chemical etching of the InP sacrificial layer in HCl solution. (c) SiO₂ spacer layer deposition by PE-CVD. (d) Transfer of a graphene sheet onto the PBE laser sample. (e) Ti/Au deposition on the graphene and glass substrate using e-gun evaporator, and epoxy bonding of the PBE laser sample on the glass substrate. (f) Transfer of an ion-gel film onto the entire device.

Laser output measured for the PBE laser

In order to determine the proper range for an electrical modulation of the PBE laser, we measured a complete performance map near laser thresholds, that is, the laser output intensity as a function of both excitation power density and gate voltage. The measured results are summarized in Fig. S2, where the peak excitation power density range was from 0.43 kW/cm^2 to 0.72 kW/cm^2 , while the gate voltage covers the range of $-1.0 \text{ V} \leq V_g < 0 \text{ V}$. As shown in Fig. S2, laser operation was not observed for $V_g > -0.5 \text{ V}$ or for the peak excitation power density below 0.45 kW/cm^2 . Otherwise, the laser output intensity monotonically increased as the gate voltage was lowered or the excitation level was increased.

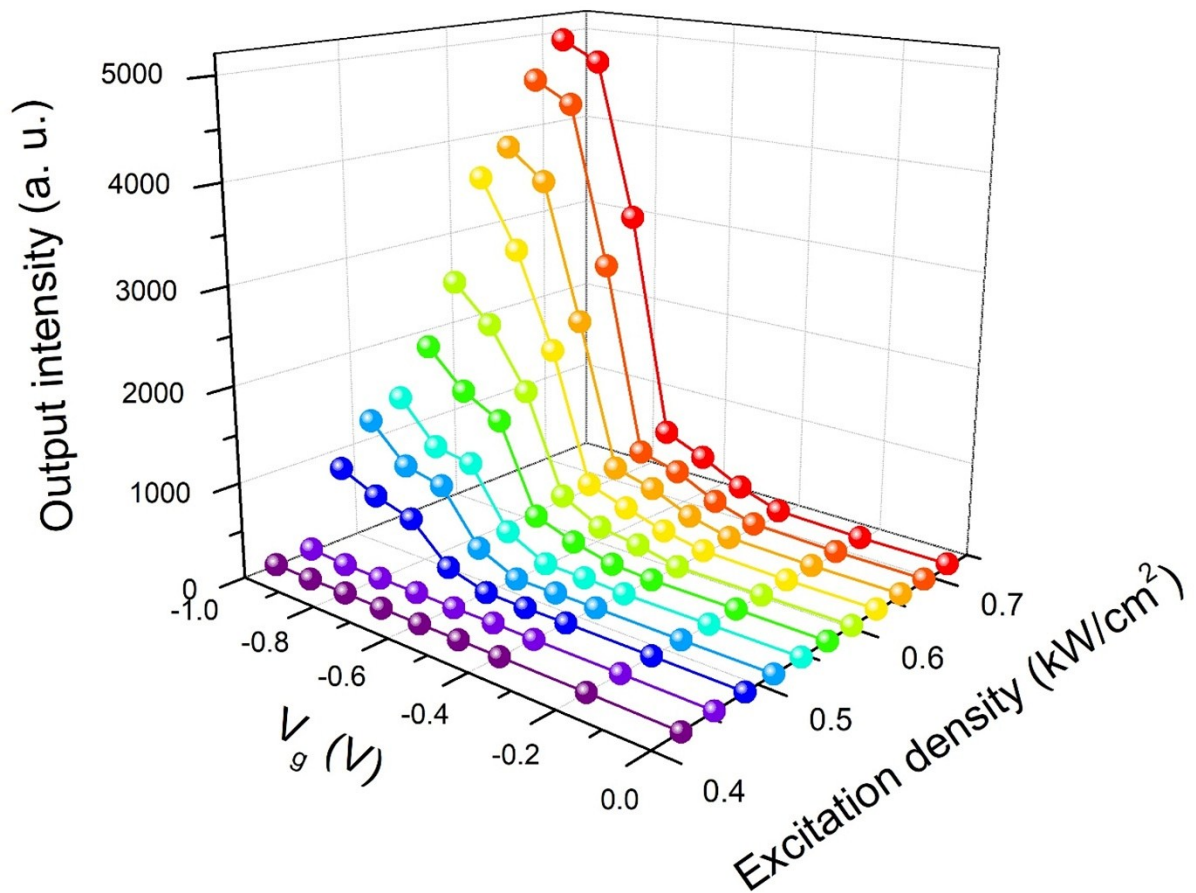


Figure S2. Measured peak output intensity of the PBE laser as a function of the peak excitation power density and the gate voltage.

Optical absorption of graphene monolayer

Optical loss of graphene can be described by optical conductivity σ .² In the Kubo formalism, the optical conductivity is contributed by both the interband and intraband transitions ($\sigma = \sigma_{inter} + \sigma_{intra}$), which can be formulated by³

$$\sigma_{inter}(\omega, \mu_c, \Gamma, T) = \frac{ie^2(\omega - i2\Gamma)}{\pi\hbar^2} \int_0^\infty \frac{f_d(-\varepsilon) - f_d(\varepsilon)}{(\omega - i2\Gamma)^2 - 4(\varepsilon/\hbar)^2} d\varepsilon \quad (1)$$

and

$$\sigma_{intra}(\omega, \mu_c, \Gamma, T) = \frac{-ie^2}{\pi\hbar^2(\omega - i2\Gamma)} \int_0^\infty \varepsilon \left(\frac{\partial f_d(\varepsilon)}{\partial \varepsilon} - \frac{\partial f_d(-\varepsilon)}{\partial \varepsilon} \right) d\varepsilon. \quad (2)$$

where $f_d(\varepsilon) = [e^{(\varepsilon - \mu_c)/k_B T} + 1]^{-1}$ is the Fermi-Dirac distribution function, ω is the angular frequency, Γ is the scattering rate, μ_c is the chemical potential, T is temperature, $-e$ is the electron charge, \hbar is the reduced Plank constant, and k_B is the Boltzmann constant.

In general, the optical absorption of a graphene monolayer occurs predominantly by the interband transition so that the optical power absorbed by graphene on the x - y plane can be expressed as

$$\langle P \rangle = \frac{1}{2} \int \mathbf{J} \cdot \mathbf{E} dx dy = \frac{\sigma_{inter}}{2} \int (|E_x|^2 + |E_y|^2) dx dy, \quad (3)$$

where \mathbf{J} is the surface current density given by Ohm's law, $\mathbf{J} = \sigma_{inter} \mathbf{E}$, and \mathbf{E} is the transverse electrical field.⁴ We calculated the transverse electric field distribution at the graphene plane of the PhC-graphene structure by FDTD simulation. Then we obtained the optical absorption in the PhC-graphene system by substituting the simulated transverse electric field distribution

of the PBE mode and the interband conductivity (1) into the power absorption equation (3).

The parameters used in the simulation are $\Gamma = 0.015$ eV,⁵ $T = 300$ K, and 0 eV $\leq \mu_c \leq 0.5$ eV.

We assumed that the thicknesses of InGaAsP slab, SiO₂ spacer layer, and ion-gel film were 230 nm, 60 nm, and 2 μ m, respectively, while their refractive indices were assumed to be 3.4, 1.4 and 1.4, respectively. Resultant optical absorption is presented in Fig. 3e as a function of gate voltage. The total absorption by graphene in the ungated state ($V_g = 0$ V) is $\sim 54\%$, which is reduced to $\sim 21\%$ at $V_g = -1.0$ V.

REFERENCES

- 1 K. Lee, M. Kang, S. Zhang, Y. Gu, T. P. Lodge and C. D. Frisbe, *Adv. Mater.*, 2012, **24**, 4457-4462.
- 2 J. M. Dawlaty, S. Shivaraman, J. Strait, P. George, M. Chandrashekhar, F. Rana, M. G. Spencer, D. Veksler and Y. Chen, *Appl. Phys. Lett.*, 2008, **93**, 131905.
- 3 G. W. Hanson, *J. Appl. Phys.*, 2008, **103**, 064302.
- 4 H. Li, Y. Anugrah, S. J. Koester and M. Li, *Appl. Phys. Lett.*, 2012, **101**, 111110.
- 5 A. Majumdar, J. Kim, J. Vuckovic, F. Wang, *Nano Lett.*, 2013, **13**, 515-518.